Liver Research 8 (2024) 269–281

Contents lists available at ScienceDirect

Liver Research

journal homepage: http://www.keaipublishing.com/en/journals/liver-research

Original Article

Kehuang capsule inhibits MAPK and AKT signaling pathways to mitigate CCl_4-induced acute liver injury

Qinyu Ni [a, b, 1], Jiacheng Lin [a, 1], Weifan Huang [a], Liu Yang [a], Ran Li [c], Tianzhi Tu [c], Guangfu He [c], Yueqiu Gao [b], Xuehua Sun [b, *], Xiaoni Kong [a, **], Xiaojun Zhu [b, ***]

[a] Central Laboratory, Shuguang Hospital Affiliated to Shanghai University of Traditional Chinese Medicine, Shanghai, China
[b] Department of Liver Disease, Shuguang Hospital Affiliated to Shanghai University of Traditional Chinese Medicine, Shanghai, China
[c] Kexing Biopharm Co., Ltd, Jinan, Shandong, China

ARTICLE INFO

Article history:
Received 2 August 2024
Received in revised form
27 September 2024
Accepted 28 November 2024

Keywords:
Kehuang capsule
Acute liver injury (ALI)
Carbon tetrachloride (CCl_4)
Mitogen-activated protein kinase (MAPK)
Protein kinase B (AKT)
Network pharmacology

ABSTRACT

Background and aims: Kehuang (KH) capsule is an herbal medical product approved for the treatment of liver diseases, including liver injury, in China. However, the mechanism is still unclear. This study aimed to elucidate the protective effects of KH capsule against carbon tetrachloride (CCl_4)-induced acute liver injury (ALI) in a murine model.

Methods: Mice were randomly divided into control, model (CCl_4), CCl_4+KH_Low and CCl_4+KH_High group. Liver enzyme levels and histological changes were assessed to evaluate liver injury. Oxidative stress markers and inflammatory cell infiltration in liver tissues were measured. Additionally, network pharmacology was employed to explore the potential mechanisms of KH capsule.

Results: KH capsule significantly reduced serum alanine aminotransferase (ALT) and aspartate aminotransferase (AST) levels, as well as the necrotic area in liver tissue. KH capsule also decreased the infiltration of macrophages and neutrophils, thereby inhibiting the expression of interleukin-6 (IL-6), tumor necrosis factor-alpha (TNF-α), and interleukin-1 beta (IL-1β). Furthermore, KH capsule decreased liver malondialdehyde (MDA) levels and increased superoxide dismutase (SOD) activity. The number of terminal deoxynucleotidyl transferase (TdT)-mediated dUTP nick-end labeling (TUNEL)-positive cells in liver tissue was also reduced. The expression of nuclear factor erythroid 2 related factor 2 (Nrf2) and heme oxygenase-1 (HO-1) proteins was significantly elevated, while the protein expression of cytochrome P450 2E1 (CYP2E1) was significantly reduced. Mass spectrometry identified genistein, galangin, wogonin, skullcapflavone II, and hispidulin as potential active ingredients of KH capsule. Network pharmacology analysis revealed enrichment in the mitogen-activated protein kinase (MAPK) and phosphatidylinositol 3-kinase (PI3K)-protein kinase B (AKT) signaling pathways. Western blot analysis confirmed that KH capsule suppressed AKT, extracellular signal-regulated kinase (ERK), and p38 signaling.

Conclusions: These findings suggest that KH capsule could exert protective effects against CCl_4-induced ALI, with the inhibition of MAPK and PI3K-AKT signaling pathways playing a crucial role in its mechanism of action.

1. Introduction

Acute liver injury (ALI) is a key pathological process during various acute liver diseases, featuring acute inflammatory response. ALI may develop into acute liver failure and system inflammatory reaction syndrome, significant contributors to mortality.[1] ALI is typically induced by exposure to drugs, chemicals, or alcohol, leading to oxidative stress, inflammatory responses, necrosis, and

* Corresponding author.
** Corresponding author.
*** Corresponding author.
E-mail addresses: susan_sxh@shutcm.edu.cn (Xuehua Sun), xiaonikong@shutcm.edu.cn (Xiaoni Kong), zhuxiaojun1978@126.com (Xiaojun Zhu).
[1] These authors contributed equally to this work and should be considered co-first authors.

https://doi.org/10.1016/j.livres.2024.11.006

apoptosis.[2] Chemical-induced liver injury is a common form of hepatic damage in clinical settings, frequently resulting in severe complications and posing substantial risks to human health.[3,4] Numerous synthetic chemical medications are currently used to alleviate liver injury. However, these treatments are associated with adverse effects, such as gastrointestinal irritation and weight gain.[5] Therefore, the advancement of innovative medications for liver injury that exhibit high efficacy and lack adverse effects is of paramount importance.

Kehuang (KH) capsule is an herbal medicinal product formulated from 16 Chinese medicinal herbs and has been approved by the Chinesse National Medical Products Administration. KH capsules are extensively utilized in clinical settings for the management of both acute and chronic liver injuries. The KH capsule formulation comprises Panax notoginseng, Rhizoma coptidis, Radix scutellariae, Phellodendron amurense, Rhei Radix et Rhizoma, Herba Hedyotis Diffusae, Lonicera hypoglauca, Fel serpentis liquidum, Calculus Bovis Artificiosus, Spi gleditsiae, Artificial Musk, Borneolum syntheticum, Radix Curcumae, Radix Saposhnikoviae divaricatae, Rhizoma Acori Talarinowii, and Radix Glycyrrhizae, which are traditionally recognized for their beneficial effects on liver health. Among these, Panax notoginseng, Rhizoma coptidis, Radix scutellariae, Phellodendron amurense, Rhei Radix et Rhizoma, Herba Hedyotis Diffusae, Lonicera hypoglauca, Fel serpentis liquidum, Calculus Bovis Artificiosus, and Artificial Musk have been demonstrated to possess anti-inflammatory, antioxidant, and antitumor properties.[6–11] Spi gleditsiae, Borneolum syntheticum, Radix Curcumae, and Rhizoma Acori Talarinowii exhibit antibacterial and anti-inflammatory characteristics.[12–15] Radix Glycyrrhizae exhibits both anti-inflammatory and detoxifying properties.[16]

Previous clinical studies have demonstrated that KH capsules effectively alleviate hyperbilirubinemia associated with viral hepatitis, cholestatic hepatitis, and chronic hepatitis B.[17–19] Although clinical practice has demonstrated the efficacy of KH capsule in mitigating liver injury and suppressing acute hepatic inflammation, the underlying mechanism of action remains unclear.

In this study, we aimed to clarify the anti-liver injury effect and investigate the underlying mechanism of KH capsule. We established CCl_4-induced ALI murine model to observe the effect of KH capsule and applied integrated network pharmacological analysis to investigate its key signaling mechanisms.

2. Materials and methods

2.1. Ethical approval

All animal procedures in this study were approved by the Institutional Animal Care and Use Committee of Shanghai University of Traditional Chinese Medicine (approval No. PZSHUTCM2409060001). All animal experiments complied with the ARRIVE guidelines and were carried out in accordance with the NIH Directive for animal experiments.

2.2. Animals, reagents and treatment

Male C57BL/6 mice (18–20 g) were purchased from the Jiesijie Research Institute (Shanghai, China). KH capsule was obtained from Kexing Biopharm Co., Ltd (Jinan, China) and CCl_4 was obtained from Sinopharm Chemical Reagent Co., Ltd (Shanghai, China). The mice were randomly divided into four groups ($n = 8$): control group, model (CCl_4) group, CCl_4+KH_Low group, and CCl_4+KH_High group. Based on previous studies and clinical using,[20] we chose the doses for the experiment. The normal human dose is considered a high dose, while half of the normal dose is designated as a low dose. These doses are then converted to mouse doses using the body surface area conversion formula for humans and mice.[21] The CCl_4+KH_Low and CCl_4+KH_High groups received 0.9 and 1.8 g/kg of KH capsule, respectively, via intragastric administration daily for one week. The control and CCl_4 groups were given equal volumes of physiological saline. One hour after the final dose, all groups except the control group were subjected to an intraperitoneal injection of a CCl_4 olive oil mixture (2 mL/kg) for ALI modeling, while the control group received olive oil only. Mice were euthanized with sodium pentobarbital 12 h post-injection, followed by sacrifice. For the analysis of serum active components, the mice were given KH capsule orally at 0.9 g/kg for three days. Blood samples were collected from the eyes of the mice 2 h after the last administration of the drug. Serum samples were collected and centrifuged at 1200 *g* for 10 min, then stored at −80 °C until subsequent analysis.

2.3. Biochemical assay

Liver injury was assessed by measuring serum levels of aspartate aminotransferase (AST) and alanine aminotransferase (ALT) using commercial test kits (#C009-2-1 and #C010-2-1, Nanjing Jiancheng Bioengineering Institute, Nanjing, China), following the manufacturer's protocols for each kit.

2.4. Histological staining

Liver samples were obtained from the mice and preserved in 4% paraformaldehyde for 24 h. These samples were then embedded in paraffin and sectioned to a thickness of 4 μm. The sections underwent a series of dewaxing and hydration steps to remove paraffin and enhance tissue exposure. This process involved sequential treatments with 100% xylene, 100% ethanol, 95% ethanol, 80% ethanol, 70% ethanol, and water. Hematoxylin and eosin (HE) staining was performed using an HE staining kit (#C0105, Beyotime, Shanghai, China), along with myeloperoxidase (MPO) staining from Cell Signaling (Boston, USA). Immunohistochemical (IHC) analysis included antigen retrieval with EDTA Antigen Retrieval Solution (#P0085, Beyotime, Shanghai, China) and blocking of endogenous peroxidase activity with Endogenous Peroxidase Blocking Buffer (#P0100A, Beyotime, Shanghai, China). Sections were then incubated overnight with primary antibodies against F4/80 (Proteintech, Chicago, USA), Nrf2 (CST, Boston, USA) and heme oxygenase-1 (HO-1) (Servicebio, Wuhan, China). Detection was carried out using horseradish peroxidase (HRP)-conjugated secondary antibodies followed by a chromogenic reaction with DAB (diaminobenzidine) buffer (Beyotime, Shanghai, China). Each stained section was imaged in three random fields, with at least three mice per group included in each experimental set. Image analysis was conducted using ImageJ software (version 1.8.0_322, Bethesda, USA).

2.5. Liver total SOD and MDA activity assay

Liver samples were dissected into fragments, immersed in PBS, and homogenized. Total superoxide dismutase (SOD) and malondialdehyde (MDA) levels were measured using the Total Superoxide Dismutase Assay Kit with nitro blue tetrazolium (NBT) (#S0109, Beyotime, Shanghai, China) and the Lipid Peroxidation MDA Assay Kit (#S0131, Beyotime, Shanghai, China), following the protocols.

2.6. Real-time qPCR

Total RNA was extracted from liver tissues using the Total RNA Extraction Kit (#RP4002, Bioteke, Wuxi, China). The RNA was then reverse transcribed with the HiScript II Q RT SuperMix with gDNA Wiper (#R222-01, Vazyme, Nanjing, China). Quantitative PCR was

performed on a QuantStudio 3 PCR Detection System (Thermo Fisher Scientific, Waltham, USA) using the SYBR Green qPCR Mix (#Q311-02, Vazyme, Nanjing, China). Gene expression levels were normalized to β-actin. The primer sequences used for this analysis are listed in Table 1.

2.7. Enzyme-linked immunosorbent assay (ELISA)

Mouse ELISA Kits (#88-7324 and #88-7064, Thermo Fisher, Waltham, USA) were used to quantify IL-6 and TNF-α levels in serum samples, following the manufacturer's instructions. The assay involves dispensing samples and standards into a 96-well plate pre-coated with antibodies specific to mouse IL-6 and TNF-α, followed by the addition of HRP-conjugated streptavidin. Color development is induced by adding a substrate solution, and the reaction is measured at 450 nm. Optical density (OD) values are converted to concentrations using a standard curve. Each sample is analyzed in triplicate, and the mean value is used for data interpretation.

2.8. Western blot

The protein was isolated from liver tissues employing RIPA Lysis Buffer (#89900, Thermo Fisher, Waltham, USA). The lysate underwent centrifugation at 13,000 *g* and 4 °C for 15 min, after which the supernatant containing protein was harvested. The purified protein was combined with 5 × loading buffer (#P0015, Beyotime, Shanghai, China) and resolved on 10% or 12.5% SDS-PAGE gels. Subsequently, the proteins were transferred onto nitrocellulose membranes, which were then blocked with 5% bovine serum albumin (BSA). The membranes were incubated with primary antibodies overnight at 4 °C, followed by incubation with secondary antibodies for 1.5 h at room temperature. Three technical repetitions were performed for each sample. The antibodies used included β-actin (Abgent, San Diego, USA), cytochrome P450 2E1 (CYP2E1; Abcam, Cambridge, UK), extracellular signal-regulated kinase (ERK; Abcam, Cambridge, UK), p-ERK (Abcam, Cambridge, UK), c-Jun N-terminal kinase (JNK; Abcam, Cambridge, UK), p-JNK (Abcam, Cambridge, UK), p38 (Abcam, Cambridge, UK), p-p38 (Abcam, Cambridge, UK), protein kinase B (AKT) (CST, Boston, USA), p-AKT (Santa Cruz, Santa Cruz, USA), Nrf2 (CST, Boston, USA), and HO-1 (Servicebio, Wuhan, China).

2.9. Sample preparation and LC-MS/MS analysis

The serum samples were thawed at 4 °C, and 100 μL aliquots were mixed with 400 μL of cold methanol/acetonitrile (1:1, v/v) to precipitate proteins. The mixture was centrifuged at 14,000 *g* for 20 min at 4 °C. The supernatant was then dried using a vacuum centrifuge. For LC-MS analysis, the dried samples were re-dissolved in 100 μL of acetonitrile/water (1:1, v/v) solvent.

LC-MS/MS analysis was performed using an ultrahigh performance liquid chromatography (UHPLC, 1290 Infinity LC, Agilent Technologies, Palo Alto, USA) and a quadrupole time-of-flight mass spectrometer (AB Sciex TripleTOF 6600, Boston, USA) at Shanghai Applied Protein Technology Co., Ltd. Samples were separated on a 2.1 mm × 100 mm ACQUITY UPLC BEH 1.7 μm column (Waters) with a gradient of 85% acetonitrile for 1 min, decreasing to 65% over 11 min, then to 40% in 0.1 min, held for 4 min, and increasing back to 85% in 0.1 min, followed by 5 min of re-equilibration. ESI conditions were: Ion Source Gas1 and Gas2 at 60, curtain gas at 30, source temperature at 600 °C, and IonSpray Voltage Floating at ±5500 V. In MS-only mode, data were acquired from 60 to 1000 Da with a 0.20 s accumulation time per spectrum. In MS/MS mode, data were acquired from 25 to 1000 Da with a 0.05 s accumulation time per spectrum. Product ion scans used information-dependent acquisition (IDA) with a collision energy of 35 V ± 15 eV and a declustering potential of 60 V (+) and −60 V (−). Raw data were converted to MzXML using ProteoWizard's msConvert and analyzed with XCMS. Peak picking used centWave m/z = 0.01 mg/mL and peakwidth = c (10, 60). Peak grouping used bw = 5 and mzwid = 0.025. CAMERA was used for annotation. Only variables with >50% nonzero values in one group were retained. Compound identification was based on accurate m/z values (<0.01 mg/mL) and MS/MS spectra compared to an in-house database. Missing data were filled using K-Nearest Neighbor, and extreme values were removed. Data were normalized for consistency.

Table 1
Primers of the genes used for qRT-PCR.

Gene	Forward primer sequence (5'–3')	Reverse primer sequence (5'–3')
IL-6	TCACAGAAGGAGTGGCTAAGGACC	ACGCACTAGGTTTGCCGAGTAGAT
TNF-α	TAGCCAGGAGGGAGAACAGA	TTTTCTGGAGGGAGATGTGG
β-actin	GTGCTATGTTGCTCTAGACTTCG	ATGCCACAGGATTCCATACC

Abbreviations: IL-6, interleukin-6; qRT-PCR, quantitative real-time polymerase chain reaction; TNF-α, tumor necrosis factor-alpha.

2.10. Network pharmacology

The active ingredients and targets of the drugs were collected as follows: The SMILES, InChI, and SDF structures of the compounds were obtained from the PubChem database (https://pubchem.ncbi.nlm.nih.gov/). These structures were imported into SuperPred, TargetNet, and SwissTargetPrediction for target prediction. The identified targets were then summarized and refined using the UniProt database. This process resulted in the final list of compound targets. The screening of drug and disease-related targets was conducted as follows: disease-related targets were extracted from GeneCards, DisGeNET, and CTD databases using the keyword "Acute Liver Injury" with specific score thresholds (GeneCards Score ≥50, DisGeNET Score ≥0.1, CTD Score ≥300). The gene names of these targets were standardized using the UniProt database. Overlapping targets among these databases were identified and visualized with a Venn diagram. The intersection of these targets with those derived from compound analysis (as described in section 2.11) was computed in R to determine the common targets, which were then considered relevant for drug treatment of ALI for subsequent analysis.

The drug-compound-target-disease network was constructed and analyzed as follows: The mapping of KH capsule active ingredients to their targets was integrated into Cytoscape (version 3.9.1, California, USA) to create a drug-compound-target-disease network diagram. In this network, nodes represent compounds and targets, while edges denote interactions between them. The Network Analyzer plugin was used to assess the network's topological characteristics and calculate node degrees. Additionally, a protein-protein interaction (PPI) network diagram was constructed using the STRING database, focusing on the overlapping targets of KH capsule in ALI. The confidence threshold was set to ≥0.95 to define protein interactions. This data was then imported into Cytoscape, where non-intersecting isolated targets were removed, and the network topology was analyzed. Core targets were identified by evaluating topological degree values (CC/BC/degree) and further refined using the MCC algorithm from the CytoHubb plugin.

The core genes linked to KH capsule and ALI were subjected to gene ontology (GO) functional enrichment analysis and Kyoto Encyclopedia of Genes and Genomes (KEGG) pathway enrichment analysis via the R clusterProfiler 4.6.2 package. For the GO analysis, bar graphs were generated to illustrate the top 20 biological

processes with a *P*-value below 0.05. In the KEGG analysis, bubble graphs were utilized to visualize the top 30 signaling pathways, also with a *P*-value less than 0.05. Drug-Compound-Target-Pathway-Disease Network Construction and Analysis. To explore the potential mechanisms of drug action, a "drug-compound-target-pathway-disease" network was constructed. This network highlights central pathways, critical targets, and active ingredients, elucidating their interconnections and synergistic interactions.

2.11. Molecular docking

The critical compounds were subjected to docking with the primary target molecules. The three-dimensional structures of the key active compounds in the drugs were sourced from the PubChem database, while the 3D structures of the core target proteins were obtained from the Protein Data Bank (https://www.rcsb.org/). The target proteins underwent preliminary processing using PyMOL (version 2.6.0, DeLano Scientific LLC, California, USA) to eliminate solvent molecules, followed by hydrogenation and charging via AutoDock Tools (version 1.5.7, San Diego, USA). Subsequently, both the target proteins and active compounds were formatted into "pdbqt" files, with suitable grid positions and dimensions established. Docking of the compounds and targets was executed using Autodock Vina (version 1.2.2, San Diego, USA), and the results were visualized using PyMOL software.

2.12. Statistical analysis

Statistical analysis was conducted using GraphPad Prism (version 9.5.1, GraphPad Software, San Diego, USA). The data were expressed as means ± standard deviation (SD). Differences among groups were compared by one-way analysis of variance (ANOVA). If a statistically significant change was found ($P < 0.05$), a post hoc comparison was performed using Fisher's LSD test.

3. Results

3.1. Kehuang capsule ameliorated CCl_4-induced liver dysfunction in mice

CCl_4 was used to establish an experimental model of ALI. The animal experiment design was illustrated in Fig. 1A. Serum levels of alanine aminotransferase (ALT) and aspartate aminotransferase (AST) were significantly elevated in the CCl_4 group, indicating successful induction of ALI. Treatment with KH capsule resulted in a significant reduction in ALT and AST levels (Fig. 1B and C). Regional liver necrosis is a characteristic histological feature observed in CCl_4-induced ALI. Hepatic HE staining showed necrotic areas with shrunken and irregularly shaped hepatocytes surrounding the hepatic sinusoids (indicated by the dashed area), confirming the successful induction of ALI in the CCl_4 group. Both doses of KH capsule reduced these necrotic areas and alleviated histological alterations, demonstrating its protective effect against CCl_4-induced liver injury (Fig. 1D and E). Moreover, the CCl_4-treated group exhibited a substantial increase in TUNEL-positive cells, which was significantly mitigated by KH capsule administration (Fig. 1F). Collectively, KH capsule treatment markedly alleviated CCl_4-induced hepatic impairment.

3.2. Kehuang capsule reduced liver oxidative in CCl_4-induced liver injury in mice

SOD activity serves as an indicator of the body's capacity to neutralize oxygen radicals, whereas MDA concentration mirrors cellular damage induced by free radicals. In the context of ALI, oxidative stress plays a pivotal role, with reactive oxygen species (ROS) contributing to cellular damage and inflammation. KH capsule treatment significantly decreased oxidative damage markers, resulting in higher SOD and lower MDA levels compared to the CCl_4 group (Fig. 2A and B). These findings indicate that KH capsule effectively mitigates oxidative stress and cellular damage. Furthermore, KH capsule markedly increased the expression of Nrf2 and HO-1, while concurrently reducing the expression of CYP2E1 (Fig. 2C–F). Changes in Nrf2 and HO-1 were also observed in the results of immunohistochemical staining (Fig. 2G–I). Nrf2 is a key transcription factor regulating antioxidant genes, including HO-1, which degrades heme into antioxidants biliverdin and bilirubin, and anti-inflammatory carbon monoxide. CYP2E1 in hepatocytes metabolizes CCl_4 to trichloromethyl radicals, which subsequently induce lipid peroxidation and result in oxidative stress. The upregulation of Nrf2 and HO-1 suggests an enhanced cellular antioxidant response, underscoring the potential of KH capsules in mitigating oxidative stress-induced liver injuries through the activation of the Nrf2/HO-1 pathway.

3.3. Kehuang capsule inhibited the liver inflammatory response

CCl_4 induces significant infiltration of macrophages and neutrophils, which are crucial for the inflammatory response. Macrophages (F4/80+) contribute to early and persistent inflammatory activation in the liver injury, while neutrophils (MPO+) release ROS and enzymes that exacerbate early tissue damage. Immunohistochemical staining showed a marked increase in F4/80+ and MPO+ cells after CCl_4 treatment (Fig. 3A–C). KH capsule significantly reduced this infiltration, indicating its anti-inflammatory effect. KH capsule also suppressed the expression of pro-inflammatory cytokines IL-1β, TNF-α, and IL-6 mRNA in the liver (Fig. 3D–F) and lowered serum levels of IL-6 and TNF-α (Fig. 3G and H). This decrease in cytokine levels underscores the role of KH capsule in alleviating inflammation and liver injury caused by CCl_4.

3.4. Identification of the components and potential target of Kehuang capsule

The UHPLC-MS/MS analysis is shown in Supplemental Fig. 1. A total of 40 compounds in the drug-containing serum, as detailed in Supplemental Table 1. The valid information of the compounds was retrieved by PubChem database, and the potential targets of the active ingredients of the compounds were predicted by SuperPred (probability ≥0.7), TargetNet (probability ≥0.7), and SwissTargetPrediction (probability >0) databases, and after deleting the target duplicates, a total of 795 compound targets were obtained (Fig. 4A).

3.5. Target network of Kehuang capsule on ALI

The CTD (score ≥350), GeneCards (score ≥50), and DisGeNET (score ≥0.2) databases were queried to identify disease-associated outcomes, with results filtered according to the specified thresholds. This process identified 751 disease targets, which were subsequently consolidated by aggregating canonical gene names and eliminating redundancy. These disease-related targets were then intersected with the 795 targets linked to the active ingredients of the KH. Following the integration of these datasets, 154 overlapping targets were identified as potential therapeutic targets for the compounds in relation to the disease. The retrieval of disease targets is shown in Fig. 4B, while the intersection of compound and disease targets is depicted in Fig. 4C.

The compound-target-disease network illustrated in Fig. 4D consists of 195 nodes and 1531 edges, where the edges represent

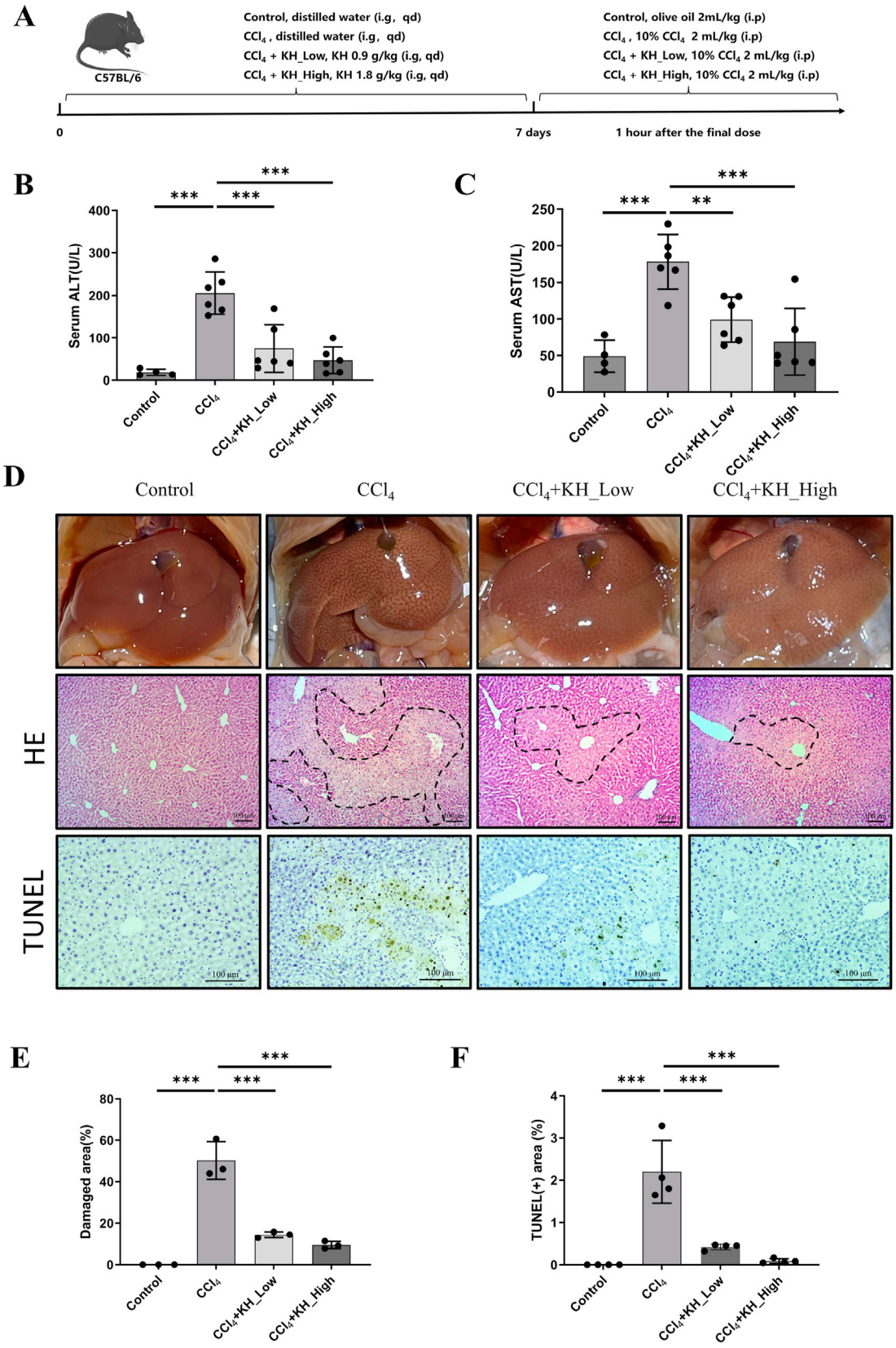

Fig. 1. KH capsule treatment ameliorates CCl_4-induced liver dysfunction in mice. **(A)** Experimental design. **(B–C)** The changes in serum ALT and AST levels ($n \geq 4$). **(D–F)** The visual inspection and quantification of necrotic areas in liver section by HE staining ($n = 3$) and TUNEL-staining ($n = 4$) and quantification of positive area in the liver section. Data are expressed as means ± standard deviation. $^{**}P < 0.01$, $^{***}P < 0.001$. Original magnification, ×100.cale bar = 100 μm. Abbreviations: ALT, alanine aminotransferase; AST, aspartate aminotransferase; CCl_4, carbon tetrachloride; HE, hematoxylin and eosin; i.g, intragastric injection; i.p, intraperitoneal injection; KH, Kehuang; TUNEL, terminal deoxynucleotidyl transferase-mediated dUTP nick-end labeling.

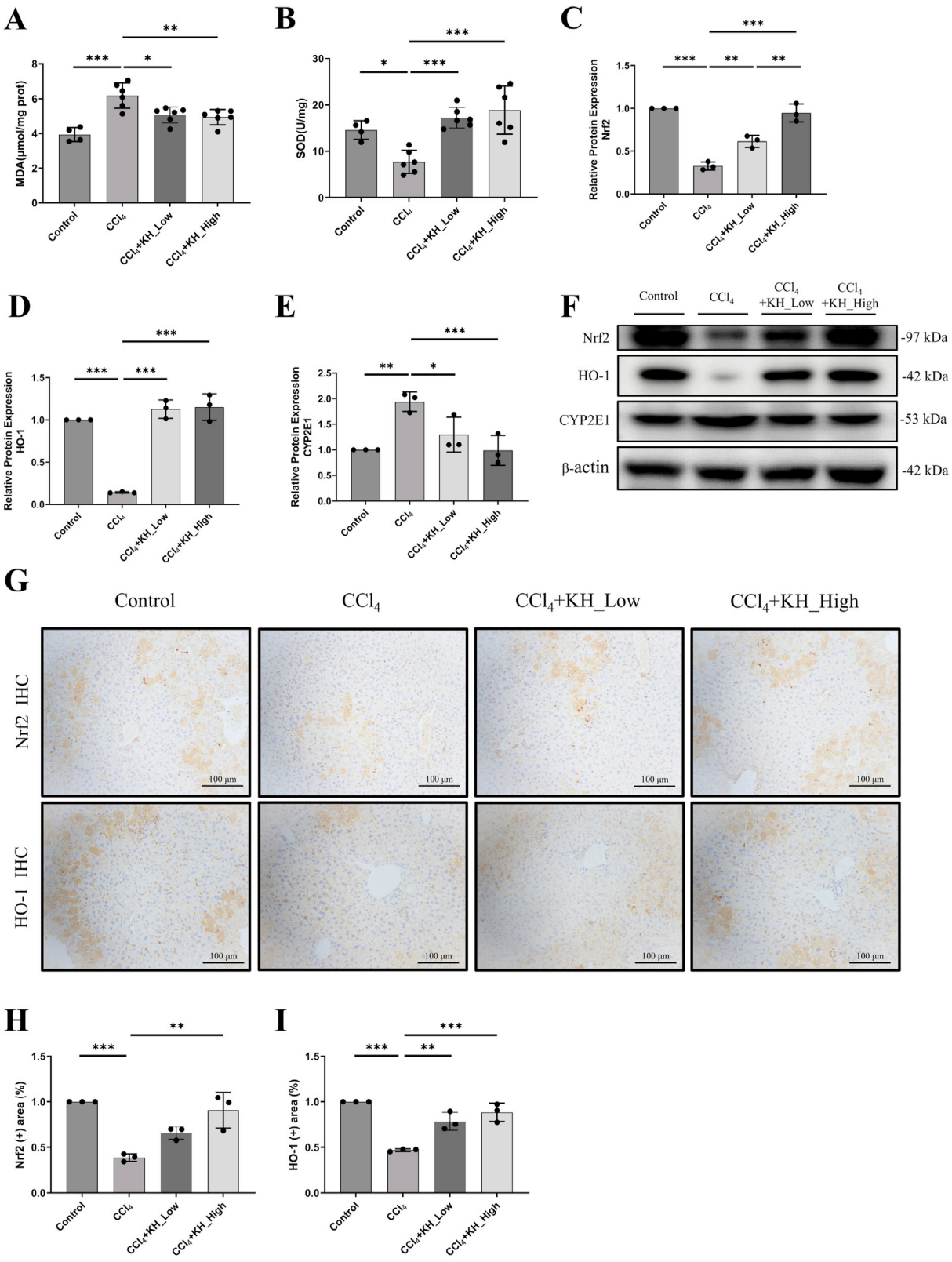

Fig. 2. KH capsule treatment reduced liver oxidative in CCl_4-induced liver injury in mice. The levels of **(A)** MDA and **(B)** SOD after CCl_4 treatment ($n \geq 4$). The statistical graphs of protein expression of **(C)** Nrf2 ($n = 3$), **(D)** HO-1 ($n = 3$), and **(E)** CYP2E1 ($n = 3$). **(F)** The protein expression of Nrf2, HO-1 and CYP2E1. **(G)** IHC staining of Nrf2 and HO-1 in the liver (Scale bar = 100 μm). **(H)** Quantification of Nrf2 (+) area ($n = 3$). **(I)** Quantification of HO-1 (+) area ($n = 3$). Data are expressed as means ± standard deviation. *$P < 0.05$, **$P < 0.01$, ***$P < 0.001$. Abbreviations: CCl_4, carbon tetrachloride; CYP2E1, cytochrome P450 2E1; HO-1, heme oxygenase-1; IHC, immunohistochemical; KH, Kehuang; MDA, malondialdehyde; Nrf2, nuclear factor erythroid 2 related factor 2; SOD, superoxide dismutase.

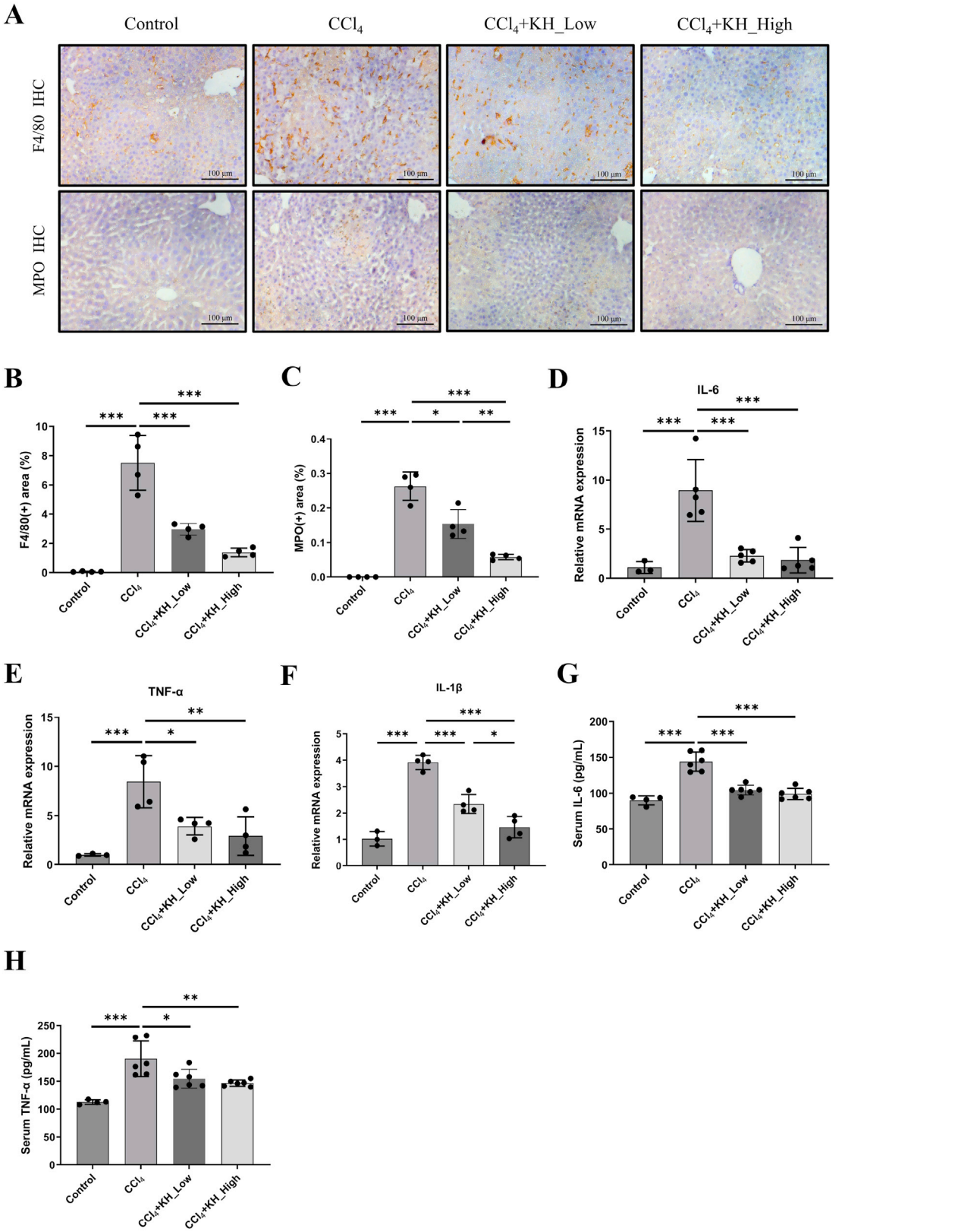

Fig. 3. KH capsule inhibited the liver inflammatory response in CCl_4-induced liver injury in mice. **(A)** Representative images of the IHC staining of F4/80 and MPO in the liver (Scale bar = 100 μm). **(B–C)** The quantification of F4/80 (+) and MPO (+) area ($n = 4$). **(D–F)** The IL-6, TNF-α and IL-1β mRNA level ($n \geq 3$). **(G–H)** The serum level of IL-6 and TNF-α ($n \geq 4$). Data are expressed as means ± standard deviation. $^*P < 0.05$, $^{**}P < 0.01$, $^{***}P < 0.001$. Abbreviations: CCl_4, carbon tetrachloride; IHC, immunohistochemical; IL, interleukin; KH, Kehuang; MPO, myeloperoxidase; TNF-α, tumor necrosis factor-alpha.

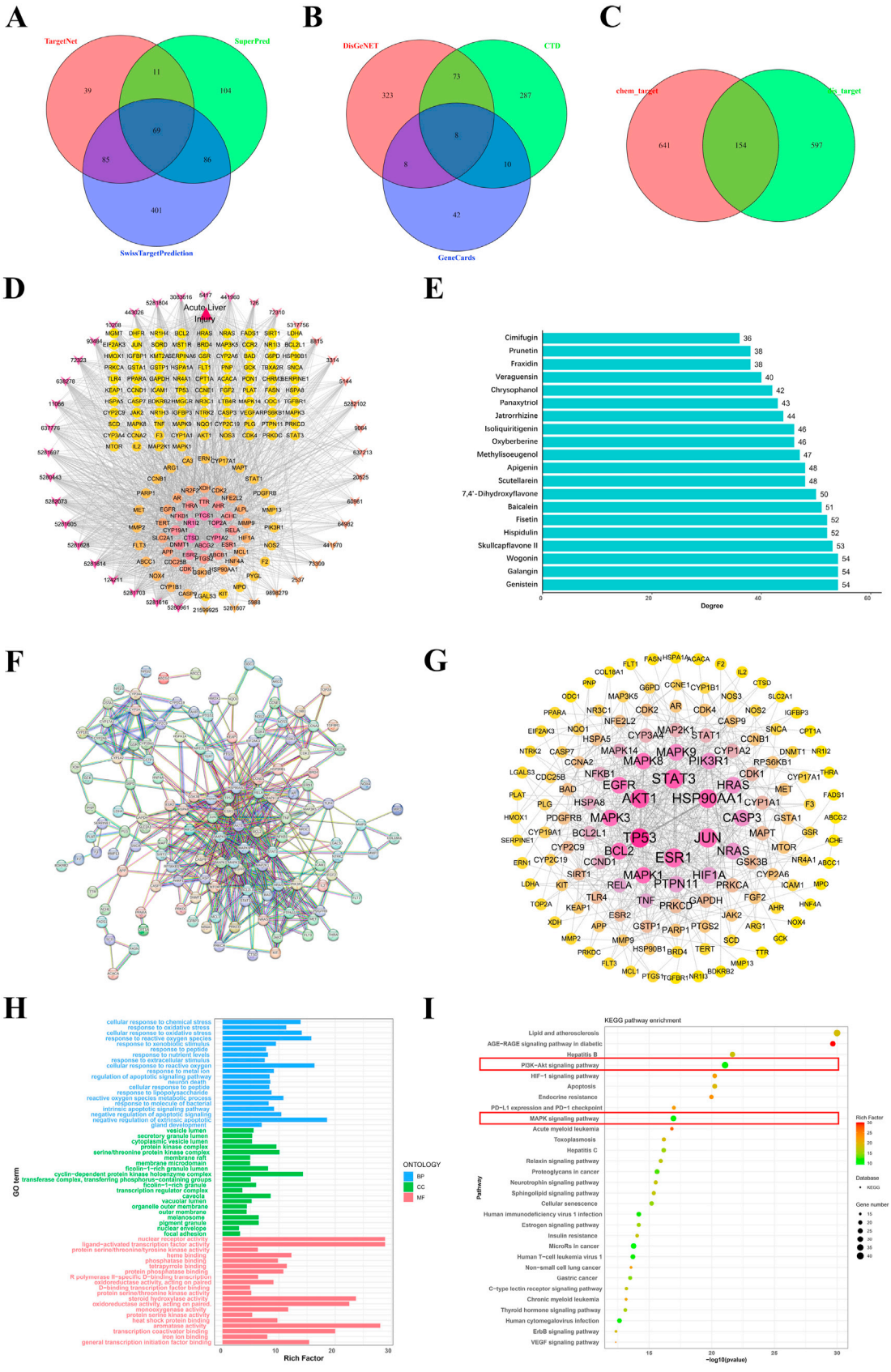

Fig. 4. Network pharmacology analysis of Kehuang capsule in the treatment of ALI. **(A)** Venn diagram of the intersection of targets between different databases. **(B)** Venn diagram of disease targets in different databases. **(C)** Venn diagram of the intersection of compound and disease targets. **(D)** Network diagram of compound-target-disease. **(E)** Histogram of the ordering of the degree values of the top 20 major components. **(F)** Diagram of STRING interaction. **(G)** Diagram of PPI interaction network. **(H)** GO enrichment

the targeting relationships between compounds and targets. This network includes 40 compounds that interact with 154 targets, which, to a certain extent, elucidates the mechanism of traditional Chinese medicine (TCM) through the interplay of various active ingredients on shared targets and the multifaceted influence of a single active ingredient on multiple targets. The topological characteristics of the network were evaluated using the Network Analyzer plugin. In the network graph, node size is proportional to the degree value, with larger degree values indicating a more central role for the node within the network. The top 20 major ingredients were ranked based on their degree values, as shown in Fig. 4E. The analysis identified genistein, galangin, wogonin, skullcapflavone II, and hispidulin as predominant active ingredients. The network graph employs different shapes to differentiate between drugs, compounds, and targets, while varying color shades denote the degree weight magnitude within the network. The STRING database was used to import and analyze the interactions of 154 compounds targeted for disease treatment, revealing protein-protein interactions (PPI) and STRING network connections (Fig. 4F). This network was subsequently processed using Cytoscape software, resulting in the graph depicted in Fig. 4G. Comprising 134 nodes and 496 edges, the graph illustrates the associations among these targets, with isolated targets lacking intersections being excluded. Prominent targets identified as pivotal for the therapeutic efficacy of KH capsule in treating ALI include TP53, AKT1, STAT3, HSP90AA1, JUN, ESR1, and MAPK1.

3.6. GO functional enrichment analysis and KEGG pathway analysis

Using the R package clusterProfiler, we conducted GO enrichment analysis on 154 overlapping targets associated with disease treatment by compounds. The top 15 significant ($P < 0.05$) GO terms for biological processes (BPs), molecular functions (MFs), and cellular components (CCs) were identified and visualized in bar plots (Fig. 4H). In these plots, the vertical axis represents each GO term, and the horizontal axis indicates the number of enriched targets. BP terms primarily included cellular responses to chemical stress and oxidative stress. MF terms were characterized by nuclear receptor activity, ligand-activated transcription factor activity, and protein serine/threonine/tyrosine kinase activity. CC terms encompassed vesicle lumen, secretory granule lumen, and cytoplasmic vesicle lumen. KEGG pathway enrichment analysis of the targets revealed 178 enriched signaling pathways. We focused on the top 30 pathways with $P < 0.05$ and visualized them using bubble diagrams (Fig. 4I). The enriched pathways primarily involved lipid and atherosclerosis, AGE-RAGE signaling pathway in diabetic complications, hepatitis B, PI3K-AKT signaling pathway, HIF-1 signaling pathway, apoptosis, endocrine resistance, PD-L1 expression and PD-1 checkpoint, and MAPK signaling pathway. These pathways exhibited synergistic interactions in disease treatment. Given that KH capsule inhibits inflammation and oxidative stress in ALI mice, we propose that the regulation of MAPK and PI3K-AKT signaling pathways is a key mechanism of KH capsule.

3.7. Molecular docking analysis revealed the potential target of Kehuang capsule

Network pharmacology has established the significance of the MAPK and PI3K-AKT signaling pathways in the therapeutic efficacy of KH capsule. To further elucidate the interaction between the KH capsule's constituents and these pathways, molecular docking studies were conducted. The top five ingredients were docked against AKT1 and MAPK1, with the resulting docking energies summarized in Table 2. A binding energy below −5 kcal/mol is indicative of a strong interaction between the active components and the target proteins. The results of the molecular docking are visually represented in Fig. 5, accompanied by annotations.

Table 2
Core targets-core compounds and their docking binding energy with AKT1 and MAPK1.

Compounds	Binding energy (kcal/mol)	
	AKT1	MAPK1
Skullcapflavone II	−7.54	−6.52
Genistein	−7.90	−7.37
Galangin	−7.99	−7.84
Hispidulin	−7.90	−7.10
Wogonin	−7.62	−7.81

Abbreviations: AKT, protein kinase B; MAPK, mitogen-activated protein kinase.

3.8. Kehuang capsule reduced inflammation via MAPK and PI3K-AKT signaling pathways in CCl_4-induced ALI

To elucidate the mechanism underlying the anti-inflammatory effects of KH capsule, we investigated the alterations in the MAPK and PI3K-AKT signaling pathways using Western blot analysis. The PI3K-AKT pathway is essential for cell survival and proliferation, and its dysregulation is frequently linked to heightened inflammation and oxidative stress. Likewise, the MAPK pathway, comprising ERK, JNK, and p38, is pivotal in modulating inflammatory responses and cell apoptosis.

Our findings demonstrated that KH capsule significantly inhibited the phosphorylation of AKT, ERK, and p38 (Fig. 6A–E). The suppression of AKT phosphorylation suggests a reduction in inflammatory signaling and oxidative stress, which in turn enhances cell survival and mitigates liver damage. The inhibition of ERK and p38 phosphorylation indicates a downregulation of the inflammatory response and apoptotic signaling pathways, both of which are pivotal in alleviating liver injury. These results suggest that the inhibition of MAPK and PI3K-AKT signaling pathways is a critical mechanism through which KH capsule ameliorates CCl_4-induced ALI.

4. Discussion

Network pharmacology, adept at elucidating multi-component, multi-target, and multi-pathway interactions, is particularly well-suited for understanding the mechanisms underlying TCM.[22] Additionally, pharmacological analysis of serum offers crucial insights into the *in vivo* transformations of herbal medicines. This study integrated network pharmacology and serum pharmacology to identify the active constituents, predicted targets, and potential mechanisms of action of KH capsule, validated through a mouse model. UHPLC analysis identified 40 compounds. Compound-target-disease network analysis suggested that genistein, galangin, wogonin, skullcapflavone II, and hispidulin might be the primary active ingredients. Genistein has been shown to alleviate acetaldehyde-induced oxidative stress and liver damage by reactivating the hepatic NRF2-HO-1 signaling pathway.[23] Galangin exhibits hepatoprotective effects in rats by mitigating oxidative stress,

analysis. **(I)** KEGG pathway. Abbreviations: AKT, protein kinase B; GO, gene ontology; HIF, hypoxia-inducible factor 1; KEGG, Encyclopedia of Gene and Genomics; PI3K, phosphatidylinositol 3-kinase; PPI, protein-protein interaction.

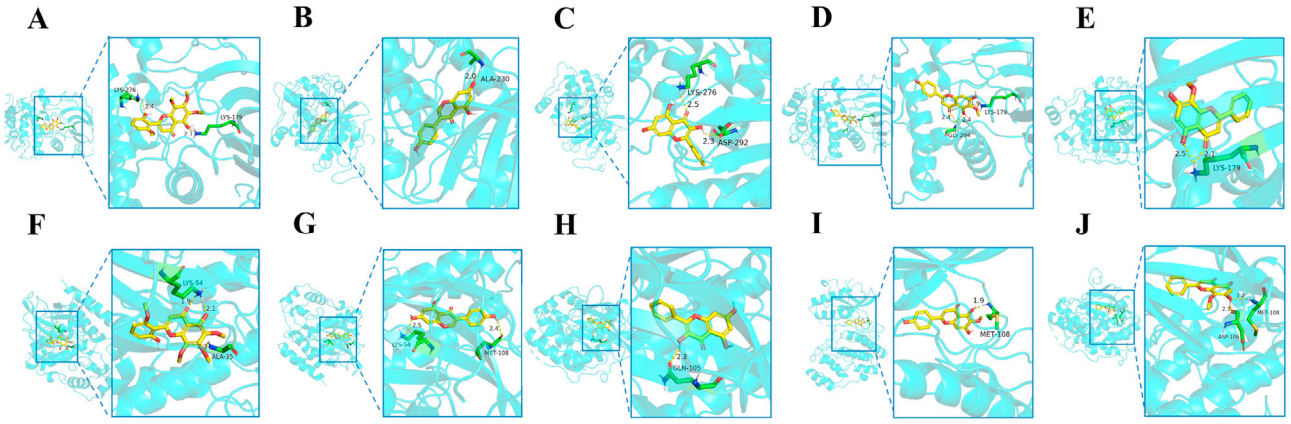

Fig. 5. Molecular docking models of Kehuang capsule with possible core anti-acute liver injury targets. AKT1 with **(A)** Skullcapflavone II, **(B)** Genistein, **(C)** Galangin, **(D)** Hispidulin, **(E)** Wogonin. MAPK1 with **(F)** Skullcapflavone II, **(G)** Genistein, **(H)** Galangin, **(I)** Hispidulin, **(J)** Wogonin. Abbreviations: AKT, protein kinase B; MAPK, mitogen-activated protein kinase.

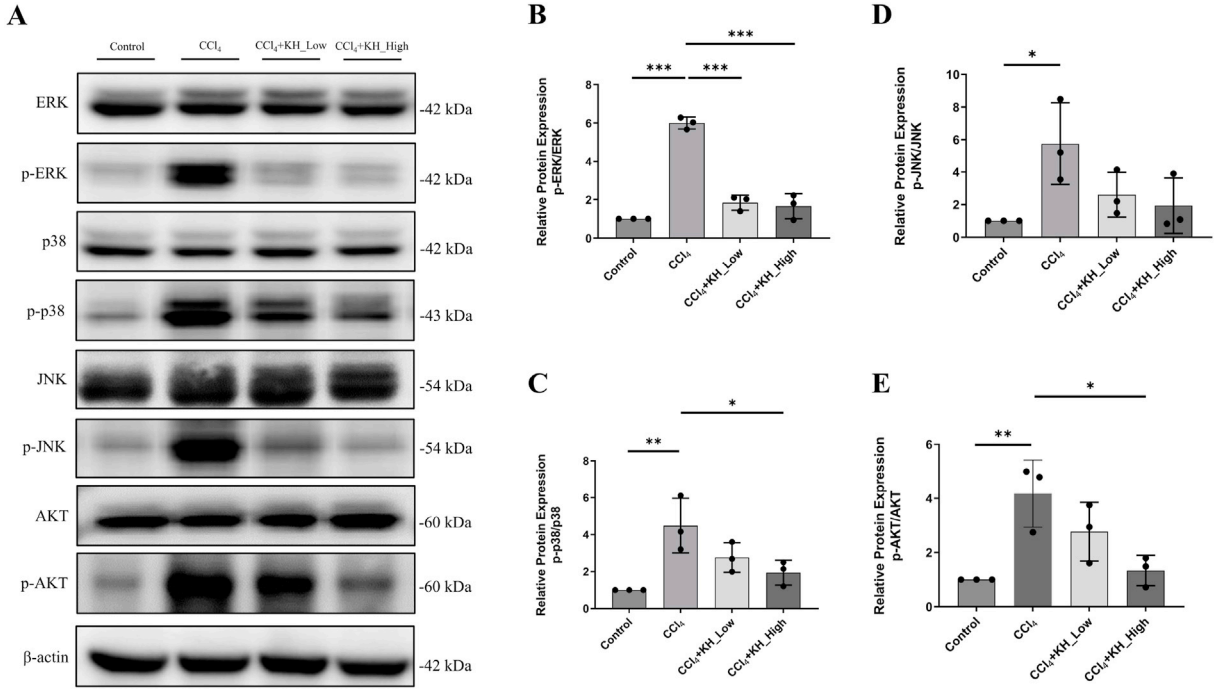

Fig. 6. KH capsule reduced inflammation via MAPK and PI3K-AKT signaling pathways in CCl_4-induced ALI. (A) The protein expression of ERK, P38, JNK, and AKT were detected using Western blotting analysis. **(B–E)** Statistical graphs of relative protein expression of ERK, P38, JNK, and AKT. Data are expressed as means ± standard deviation ($n = 3$). $^*P < 0.05$, $^{**}P < 0.01$, $^{***}P < 0.001$. Abbreviations: AKT, protein kinase B; CCl_4, carbon tetrachloride; ERK, extracellular signal-regulated kinase; JNK, c-Jun N-terminal kinase; KH, Kehuang.

inflammation, and apoptosis.[24] Wogonin has been demonstrated to therapeutically intervene in acetaminophen (APAP)-induced liver injury in mice by suppressing macrophage inflammatory responses through the inhibition of the PI3K-AKT signaling pathway.[25] Skullcapflavone II has been associated with antioxidant activities, while hispidulin is recognized as a natural anticancer compound.[26] KEGG pathway analysis demonstrated significant enrichment of the MAPK and PI3K-AKT signaling pathways, which are crucial in liver injury.[27,28] Activation of the MAPK signaling pathway enhances early inflammatory responses, resulting in elevated expression of pro-inflammatory cytokines including IL-6, IL-1β, and TNF-α, which subsequently promote apoptosis in cells.[29] During ALI, the activation of PI3K-AKT signaling pathway is implicated in the production of inflammatory factors and hepatocyte apoptosis.[30] These network pharmacology predictions were corroborated using the CCl_4-induced ALI model in mice.

Current research indicates that ALI induced by CCl_4 exhibits symptoms strikingly similar to those seen in human liver injury,[31–35] including hepatocyte necrosis, inflammatory responses, and oxidative stress. These features render the CCl_4-induced ALI model highly valuable for mimicking human liver injury, thereby making it widely utilized in the development and study of ALI models. Our results demonstrate that KH capsule effectively alleviates CCl_4-induced ALI. Treatment with KH capsule significantly reduced the elevated serum aminotransferase activities, protected hepatocytes, and preserved their structural

integrity in mice exposed to CCl_4. Histological analysis using F4/80 staining revealed a marked increase in liver macrophage infiltration 12 h post-CCl_4 injection, which was mitigated by pretreatment with KH capsule. An increase in liver macrophage count is a well-recognized hallmark of liver injury.[36] In the context of ALI, the influx of peripheral monocytes can differentiate into macrophages, resulting in a significant increase in the number of macrophages within the liver.[37,38] Our findings provide evidence that KH capsule exerts a suppressive effect on hepatic inflammatory infiltration.

Liver injury is marked by the infiltration of macrophages and a significant increase in pro-inflammatory cytokines, including TNF-α and IL-6. This inflammatory response exacerbates hepatocyte damage and cell death through elevated cytokine levels and the production of ROS by inflammatory cells.[39] The inflammatory response elicited by CCl_4 is primarily mediated by the overproduction of pro-inflammatory cytokines such as IL-6, IL-1β, and TNF-α.[33] Our results demonstrate that serum levels of pro-inflammatory cytokines were significantly elevated in mice treated with CCl_4, but this elevation was mitigated by KH capsule administration. These findings highlight the role of KH capsule pretreatment in attenuating macrophage infiltration and decreasing pro-inflammatory cytokine production, thereby modulating liver inflammation.

Hepatotoxicity induced by CCl_4 exposure is primarily driven by oxidative stress-mediated liver injury.[40] This is commonly marked by abnormal levels of MDA and a decrease in SOD activity, indicating impaired antioxidant defense.[41] The administration of KH capsule resulted in a reduction of MDA and an increase in SOD, indicating that the KH capsule can alleviate CCl_4-induced oxidative stress. Additionally, CCl_4-induced ALI is known to trigger extensive hepatocyte apoptosis.[42] The TUNEL assay revealed a marked reduction in TUNEL-positive cells in the livers of KH capsule-treated mice, suggesting that KH capsule effectively mitigates hepatocyte apoptosis and thereby ameliorates liver injury.

Nrf2 is a key redox regulator that activates the gene expression of multiple antioxidant enzymes, effectively scavenging harmful free radicals and reducing oxidative damage to cell structure and function.[43] Previous research has demonstrated that activating Nrf2 can effectively mitigate liver damage.[44,45] Our findings indicate that exposure to CCl_4 significantly decreased Nrf2 expression in the liver, a reduction that was ameliorated by pretreatment with KH capsule. Additionally, CCl_4 exposure led to a decrease in HO-1 expression, which was also reversed by KH capsule administration. HO-1 has been shown to exert a protective effect in various experimental models of inflammation and oxidative damage,[46] and is thought to safeguard liver cells from damage induced by ALI and other etiologies.[47] Hepatotoxicity induced by CCl_4 is mediated by CYP2E1, which metabolizes CCl_4 into trichloromethyl radicals, leading to liver injury.[48] Our results indicate that KH decreases the expression of CYP2E1. These results suggest that KH capsule can alleviate hepatic oxidative stress by enhancing the Nrf2 and HO-1-mediated antioxidant defense mechanism.

The MAPK signaling pathway, comprising the ERK, JNK, and p38 subfamilies,[49,50] is pivotal in the phosphorylation of inflammatory mediators, leading to liver inflammation. This pathway is implicated in oxidative stress and inflammation, with excessive activation resulting in cellular damage.[51–53] During the process of ALI induced by CCl_4, the MAPK signaling pathway is significantly activated.[54] CCl_4 is metabolized in the liver into free radical substances, such as CCl_3 and CCl_3OO, which attack polyunsaturated fatty acids on the membranes of hepatocytes and mitochondria, triggering lipid peroxidation reactions, leading to membrane damage and increased permeability.[55] In this process, key molecules in the MAPK signaling pathway, such as ERK, JNK, and p38, are activated and participate in regulating cellular oxidative stress, the release of inflammatory factors TNF-α and IL-6, and apoptosis in hepatocytes. In our study, CCl_4 treatment significantly elevated the expression of ERK, JNK, and p38, which could be reduced by KH capsule. This suggests that KH capsule mitigates CCl_4-induced MAPK signaling activation. Additionally, the initiation and progression of hepatic damage have been linked to the PI3K-AKT pathway. KH capsule decreased the phosphorylation level of AKT. This indicates that KH capsule may be through the PI3K-AKT pathway to alleviate CCl_4-induced liver damage.

In summary, KH capsule demonstrated the inhibition of liver necrosis, as well as a reduction in inflammation and oxidative stress in mice, potentially through the suppression of the MAPK and AKT pathways, thereby reversing the majority of pathological alterations associated with CCl_4-induced liver injury. These results lay a solid groundwork for the potential clinical application of KH capsule in ALI. However, this study has certain limitations, as it only utilized one ALI model without verification at the cellular level. Regarding the relevance of KH capsule pretreatment, we acknowledge that routine use of KH capsule before hepatotoxin exposure may not reflect a common clinical scenario. However, pretreatment models can be used to assess potential protective effects.[56,57] In real-world applications, KH capsule could be beneficial in scenarios where there is a known risk of hepatotoxin exposure, such as occupational settings or chronic exposure to environmental toxins.

5. Conclusions

In this study, we found that KH capsule could mitigate CCl_4-induced ALI. We suggest that KH capsule possess anti-inflammatory and antioxidant effects. The protective effect of KH capsule is potentially mediated by the suppression of the MAPK and PI3K-AKT signaling pathways.

Data availability statement

The data that support the findings of this study are available on request from the corresponding authors. The data are not publicly available due to privacy or ethical restrictions.

Authors' contributions

Qinyu Ni and Jiacheng Lin contributed equally to this work and should be considered co-first authors. **Qinyu Ni:** Investigation. **Jiacheng Lin:** Methodology. **Weifan Huang:** Validation. **Liu Yang:** Methodology. **Ran Li:** Supervision. **Tianzhi Tu:** Supervision. **Guangfu He:** Supervision. **Yueqiu Gao:** Resources, Funding acquision. **Xuehua Sun:** Conceptualization. **Xiaoni Kong:** Conceptualization. **Xiaojun Zhu:** Conceptualization. All authors approved the final version of this manuscript.

Declaration of competing interest

The authors declare the following financial interests/personal relationships which may be considered as potential competing interests: Ran Li, Tianzhi Tu and Guangfu He are currently employed by the market center of Kexing Biopharm Co., Ltd. The medicines provided by Kexing Biopharm Co., Ltd ensured the smooth conduct of the study. The opinions expressed in this study are those of the authors and do not necessarily represent those of Kexing Biopharm Co., Ltd. All researchers retained complete independence in the conduct of this study. The company had no influence on the results of the study. Other authors declare that there are no competing interests.

Acknowledgements

This work was supported by the grant from the Shanghai Famous Old Chinese Medicine Academic Research Studio (No. SHGZS-202246).

Appendix A. Supplementary data

Supplementary data to this article can be found online at https://doi.org/10.1016/j.livres.2024.11.006.

References

1. Dai C, Zhang X, Lin J, Shen J. Nootkatone supplementation ameliorates carbon tetrachloride-induced acute liver injury via the inhibition of oxidative stress, NF-κB pathways, and the activation of Nrf2/HO-1 pathway. *Antioxidants (Basel)*. 2023;12:194. https://doi.org/10.3390/antiox12010194.
2. Xin C, Liu S, Qu H, Wang Z. The novel nanocomplexes containing deoxycholic acid-grafted chitosan and oleanolic acid displays the hepatoprotective effect against CCl_4-induced liver injury in vivo. *Int J Biol Macromol*. 2021;185:338–349. https://doi.org/10.1016/j.ijbiomac.2021.06.109.
3. Meng X, Tang GY, Liu PH, Zhao CJ, Liu Q, Li HB. Antioxidant activity and hepatoprotective effect of 10 medicinal herbs on CCl_4-induced liver injury in mice. *World J Gastroenterol*. 2020;26:5629–5645. https://doi.org/10.3748/wjg.v26.i37.5629.
4. Chang SN, Kim SH, Dey DK, et al. 5-O-Demethylnobiletin alleviates CCl_4-induced acute liver injury by equilibrating ROS-mediated apoptosis and autophagy induction. *Int J Mol Sci*. 2021;22:1083. https://doi.org/10.3390/ijms22031083.
5. Wang B, Cui S, Mao B, et al. Cyanidin alleviated CCl_4-induced acute liver injury by regulating the Nrf2 and NF-κB signaling pathways. *Antioxidants (Basel)*. 2022;11:2383. https://doi.org/10.3390/antiox11122383.
6. Xie W, Meng X, Zhai Y, et al. Panax notoginseng saponins: a review of its mechanisms of antidepressant or anxiolytic effects and network analysis on phytochemistry and pharmacology. *Molecules*. 2018;23:940. https://doi.org/10.3390/molecules23040940.
7. Xu Z, Feng W, Shen Q, et al. Rhizoma coptidis and berberine as a natural drug to combat aging and aging-related diseases via anti-oxidation and AMPK activation. *Aging Dis*. 2017;8:760–777. https://doi.org/10.14336/AD.2016.0620.
8. Banik K, Khatoon E, Harsha C, et al. Wogonin and its analogs for the prevention and treatment of cancer: a systematic review. *Phytother Res*. 2022;36:1854–1883. https://doi.org/10.1002/ptr.7386.
9. Park EK, Rhee HI, Jung HS, et al. Antiinflammatory effects of a combined herbal preparation (RAH13) of Phellodendron amurense and Coptis chinensis in animal models of inflammation. *Phytother Res*. 2007;21:746–750. https://doi.org/10.1002/ptr.2156.
10. Kumar AP, Bhaskaran S, Ganapathy M, et al. Akt/cAMP-responsive element binding protein/cyclin D1 network: a novel target for prostate cancer inhibition in transgenic adenocarcinoma of mouse prostate model mediated by Nexrutine, a Phellodendron amurense bark extract. *Clin Cancer Res*. 2007;13:2784–2794. https://doi.org/10.1158/1078-0432.CCR-06-2974.
11. Yu ZJ, Xu Y, Peng W, et al. Calculus bovis: a review of the traditional usages, origin, chemistry, pharmacological activities and toxicology. *J Ethnopharmacol*. 2020;254:112649. https://doi.org/10.1016/j.jep.2020.112649.
12. Lim JC, Park JH, Budesinsky M, et al. Antimutagenic constituents from the thorns of Gleditsia sinensis. *Chem Pharm Bull (Tokyo)*. 2005;53:561–564. https://doi.org/10.1248/cpb.53.561.
13. Zhou L, Li D, Wang J, et al. Antibacterial phenolic compounds from the spines of Gleditsia sinensis Lam. *Nat Prod Res*. 2007;21:283–291. https://doi.org/10.1080/14786410701192637.
14. Wen J, Yang Y, Hao J. Acori Tatarinowii Rhizoma: a comprehensive review of its chemical composition, pharmacology, pharmacokinetics and toxicity. *Front Pharmacol*. 2023;14:1090526. https://doi.org/10.3389/fphar.2023.1090526.
15. Ao M, Li X, Liao Y, et al. Curcumae Radix: a review of its botany, traditional uses, phytochemistry, pharmacology and toxicology. *J Pharm Pharmacol*. 2022;74:779–792. https://doi.org/10.1093/jpp/rgab126.
16. Li N, Zhou T, Wu F, et al. Pharmacokinetic mechanisms underlying the detoxification effect of Glycyrrhizae Radix et Rhizoma (Gancao): drug metabolizing enzymes, transporters, and beyond. *Expert Opin Drug Metab Toxicol*. 2019;15:167–177. https://doi.org/10.1080/17425255.2019.1563595.
17. Zhang X, Guo X. 54 cases of viral hepatitis hyperbilirubinaemia treated with Kehuang capsules (in Chinese). *Chin J Integr Tradit West Med Liver Dis*. 2001;11:45–46.
18. Xie W, Chen S. Clinical retrospective study of kehuang capsule on cholestatic hepatitis (in Chinese). *J Qingyuan Polytech*. 2020;13:46–50.
19. Guo W, Chen D. Observation on the therapeutic effect of 43 cases of chronic hepatitis B in the treatment of moderate chronic hepatitis B by Kehuang capsule (in Chinese). *Chin Tradit Patent Med*. 1997;19:28–29.
20. Li X, Liu Y, Li R, Tu T, Hu Y. Pharmacodynamic study of kehuang capsules in the treatment of non-alcoholic steatohepatitis in mice (in Chinese). *Chin J Integr Tradit West Med Liver Dis*. 2024;34:230–235. https://doi.org/10.3969/j.issn.1005-0264.2024.003.009.
21. U.S. Department of Health and Human Services Food and Drug Administration Center for Drug Evaluation and Research (CDER). *Guidance for industry: estimating the maximum safe starting dose in initial clinical trials for therapeutics in adult healthy volunteers*; 2005. https://www.fda.gov/media/72309/download.
22. Qi X, Xu H, Zhang P, et al. Investigating the mechanism of Scutellariae barbata Herba in the treatment of colorectal cancer by network pharmacology and molecular docking. *Evid Based Complement Alternat Med*. 2021;2021:3905367. https://doi.org/10.1155/2021/3905367.
23. Ding Q, Pi A, Hao L, et al. Genistein protects against acetaldehyde-induced oxidative stress and hepatocyte injury in chronic alcohol-fed mice. *J Agric Food Chem*. 2023;71:1930–1943. https://doi.org/10.1021/acs.jafc.2c05747.
24. Alfwuaires MA. Galangin mitigates oxidative stress, inflammation, and apoptosis in a rat model of methotrexate hepatotoxicity. *Environ Sci Pollut Res Int*. 2022;29:20279–20288. https://doi.org/10.1007/s11356-021-16804-z.
25. Zhao W, Luo H, Lin Z, et al. Wogonin mitigates acetaminophen-induced liver injury in mice through inhibition of the PI3K/AKT signaling pathway. *J Ethnopharmacol*. 2024;332:118364. https://doi.org/10.1016/j.jep.2024.118364.
26. Ashaq A, Maqbool MF, Maryam A, et al. Hispidulin: a novel natural compound with therapeutic potential against human cancers. *Phytother Res*. 2021;35:771–789. https://doi.org/10.1002/ptr.6862.
27. Tang N, Zhang YP, Ying W, Yao XX. Interleukin-1β upregulates matrix metalloproteinase-13 gene expression via c-Jun N-terminal kinase and p38 MAPK pathways in rat hepatic stellate cells. *Mol Med Rep*. 2013;8:1861–1865. https://doi.org/10.3892/mmr.2013.1719.
28. Jing ZT, Liu W, Xue CR, et al. AKT activator SC79 protects hepatocytes from TNF-α-mediated apoptosis and alleviates d-Gal/LPS-induced liver injury. *Am J Physiol Gastrointest Liver Physiol*. 2019;316:G387–G396. https://doi.org/10.1152/ajpgi.00350.2018.
29. Dong N, Li X, Xue C, et al. Astragalus polysaccharides alleviates LPS-induced inflammation via the NF-κB/MAPK signaling pathway. *J Cell Physiol*. 2020;235:5525–5540. https://doi.org/10.1002/jcp.29452.
30. Leng J, Wang Z, Fu CL, et al. NF-κB and AMPK/PI3K/Akt signaling pathways are involved in the protective effects of Platycodon grandiflorum saponins against acetaminophen-induced acute hepatotoxicity in mice. *Phytother Res*. 2018;32:2235–2246. https://doi.org/10.1002/ptr.6160.
31. Sun Y, Demagny H, Faure A, et al. Asparagine protects pericentral hepatocytes during acute liver injury. *J Clin Invest*. 2023;133:e163508. https://doi.org/10.1172/JCI163508.
32. Wei YY, Wang HR, Fan YM, et al. Acute liver injury induced by carbon tetrachloride reversal by Gandankang aqueous extracts through nuclear factor erythroid 2-related factor 2 signaling pathway. *Ecotoxicol Environ Saf*. 2023;251:114527. https://doi.org/10.1016/j.ecoenv.2023.114527.
33. Yan JK, Wang C, Chen TT, Li L, Liu X, Li L. Structural characteristics and ameliorative effect of a polysaccharide from Corbicula fluminea industrial distillate against acute liver injury induced by CCl_4 in mice. *Int J Bio Macromol*. 2023;227:391–404. https://doi.org/10.1016/j.ijbiomac.2022.12.138.
34. Yang G, Li S, Jin J, et al. Protective effects of Longhu Rendan on chronic liver injury and fibrosis in mice. *Liver Res*. 2022;6:93–102. https://doi.org/10.1016/j.livres.2021.05.002.
35. Abdelsalam MM, El-Mahdy N, Abou-Saif S. Direct-acting antivirals sofosbuvir and daclatasvir attenuate carbon tetrachloride-induced liver fibrosis in mice. *Liver Res*. 2023;7:71–81. https://doi.org/10.1016/j.livres.2023.02.001.
36. Luo W, Ye L, Hu XT, et al. MD2 deficiency prevents high-fat diet-induced AMPK suppression and lipid accumulation through regulating TBK1 in non-alcoholic fatty liver disease. *Clin Transl Med*. 2022;12:e777. https://doi.org/10.1002/ctm2.777.
37. Karlmark KR, Weiskirchen R, Zimmermann HW, et al. Hepatic recruitment of the inflammatory Gr1+ monocyte subset upon liver injury promotes hepatic fibrosis. *Hepatology*. 2009;50:261–274. https://doi.org/10.1002/hep.22950.
38. Holt MP, Cheng L, Ju C. Identification and characterization of infiltrating macrophages in acetaminophen-induced liver injury. *J Leukoc Biol*. 2008;84:1410–1421. https://doi.org/10.1189/jlb.0308173.
39. Koyama Y, Brenner DA. Liver inflammation and fibrosis. *J Clin Invest*. 2017;127:55–64. https://doi.org/10.1172/JCI88881.
40. Zhang JQ, Shi L, Xu XN, et al. Therapeutic detoxification of quercetin against carbon tetrachloride-induced acute liver injury in mice and its mechanism. *J Zhejiang Univ Sci B*. 2014;15:1039–1047. https://doi.org/10.1631/jzus.B1400104.
41. Cai H, Xie Z, Liu G, et al. Isolation, identification and activities of natural antioxidants from Callicarpa kwangtungensis Chun. *PLoS One*. 2014;9:e93000. https://doi.org/10.1371/journal.pone.0093000.
42. Yang BY, Zhang XY, Guan SW, Hua ZC. Protective effect of procyanidin B2 against CCl_4-induced acute liver injury in mice. *Molecules*. 2015;20:12250–12265. https://doi.org/10.3390/molecules200712250.
43. Wang Y, Chen P, Chen X, et al. ROS-induced DCTPP1 upregulation contributes to cisplatin resistance in ovarian cancer. *Front Mol Biosci*. 2022;9:838006. https://doi.org/10.3389/fmolb.2022.838006.
44. Li R, Zhang P, Li C, Yang W, Yin Y, Tao K. Tert-butylhydroquinone mitigates carbon tetrachloride induced hepatic injury in mice. *Int J Med Sci*. 2020;17:2095–2103. https://doi.org/10.7150/ijms.45842.
45. Li R, Yang W, Yin Y, Ma X, Zhang P, Tao K. 4-OI attenuates carbon tetrachloride-induced hepatic injury via regulating oxidative stress and the inflammatory

response. *Front Pharmacol*. 2021;12:651444. https://doi.org/10.3389/fphar.2021.651444.
46. Belcher JD, Young M, Chen C, et al. MP4CO, a pegylated hemoglobin saturated with carbon monoxide, is a modulator of HO-1, inflammation, and vaso-occlusion in transgenic sickle mice. *Blood*. 2013;122:2757–2764. https://doi.org/10.1182/blood-2013-02-486282.
47. Du J, Ren W, Zhang Q, et al. Heme oxygenase-1 suppresses wnt signaling pathway in nonalcoholic steatohepatitis-related liver fibrosis. *Biomed Res Int*. 2020;2020:4910601. https://doi.org/10.1155/2020/4910601.
48. Zhao H, Li H, Feng Y, et al. Mycelium polysaccharides from termitomyces albuminosus attenuate CCl_4-induced chronic liver injury via inhibiting TGFβ1/Smad3 and NF-κB signal pathways. *Int J Mol Sci*. 2019;20:4872. https://doi.org/10.3390/ijms20194872.
49. Bai D, Sun T, Lu F, et al. Eupatilin suppresses OVA-induced asthma by inhibiting NF-κB and MAPK and activating Nrf2 signaling pathways in mice. *Int J Mol Sci*. 2022;23:1582. https://doi.org/10.3390/ijms23031582.
50. Li J, Li Q, Wu Q, et al. Exopolysaccharides of Lactobacillus rhamnosus GG ameliorate Salmonella typhimurium-induced intestinal inflammation via the TLR4/NF-κB/MAPK pathway. *J Anim Sci Biotechnol*. 2023;14:23. https://doi.org/10.1186/s40104-023-00830-7.
51. Frazier WJ, Xue J, Luce WA, Liu Y. MAPK signaling drives inflammation in LPS-stimulated cardiomyocytes: the route of crosstalk to G-protein-coupled receptors. *PLoS One*. 2012;7:e50071. https://doi.org/10.1371/journal.pone.0050071.
52. Liu XM, Peyton KJ, Shebib AR, Wang H, Durante W. Compound C stimulates heme oxygenase-1 gene expression via the Nrf2-ARE pathway to preserve human endothelial cell survival. *Biochem Pharmacol*. 2011;82:371–379. https://doi.org/10.1016/j.bcp.2011.05.016.
53. Li Z, Xiao W, Xie J, et al. Isolation, characterization and antioxidant activity of yam polysaccharides. *Foods*. 2022;11:800. https://doi.org/10.3390/foods11060800.
54. Ma JQ, Ding J, Zhang L, Liu CM. Ursolic acid protects mouse liver against CCl_4-induced oxidative stress and inflammation by the MAPK/NF-κB pathway. *Environ Toxicol Pharmacol*. 2014;37:975–983. https://doi.org/10.1016/j.etap.2014.03.011.
55. Feng JY, Xie YQ, Zhang P, et al. Hepatoprotective polysaccharides from geranium wilfordii: purification, structural characterization, and their mechanism. *Molecules*. 2022;27:3602. https://doi.org/10.3390/molecules27113602.
56. Shen Y, Shen X, Cheng Y, Liu Y. Myricitrin pretreatment ameliorates mouse liver ischemia reperfusion injury. *Int Immunopharmacol*. 2020;89:107005. https://doi.org/10.1016/j.intimp.2020.107005.
57. Lu J, Wang X, Feng Z, Chen Y, Wen D, Liu Z. The protective effect of isoflurane pretreatment on liver IRI by suppressing noncanonical pyroptosis of liver macrophages. *Int Immunopharmacol*. 2021;99:107977. https://doi.org/10.1016/j.intimp.2021.107977.